Spin-dependent correlations and thermodynamic functions for electron liquids at arbitrary degeneracy and spin polarization

Shigenori Tanaka and Setsuo Ichimaru
Department of Physics, University of Tokyo, 7-3-1 Hongo, Bunkyo-ku, Tokyo 113, Japan
(Received 16 November 1987; revised manuscript received 12 September 1988)

We solve a set of coupled integral equations obtained in the modified-convolution approximation scheme, to calculate the spin-dependent correlation functions and interaction energies for electron liquids at arbitrary degrees of Fermi degeneracy and spin polarization. Analytic expressions for the free energies are obtained through parametrization of the numerical results over a wide range of density, temperature, and spin polarization in the fluid state; Fermi-liquid properties are thereby investigated. Phase boundary curves, arising from divergence of the isothermal compressibility and of the spin susceptibility, are drawn on the density-temperature plane for the metallic electrons. In particular, it is pointed out that the signs and magnitudes of the spin-dependent or phonon-induced electron interactions exhibit remarkable changes across the phase boundaries; strong attractive interaction between electrons with parallel spins appears near the spin-susceptibility anomaly, where the spin-density fluctuations are enormously enhanced.

I. INTRODUCTION

The thermodynamic properties of electron liquids such as the conduction electrons in metallic substances may be determined on specifications of the average number density n or

$$r_s=\left[\frac{3}{4\pi n}\right]^{1/3}\frac{me^2}{\hbar^2}\ , \tag{1}$$

the reduced temperature

$$\Theta=k_BT\frac{2m}{\hbar^2(3\pi^2n)^{2/3}}\ , \tag{2}$$

and the spin polarization

$$\zeta=(n_1-n_2)/n\ . \tag{3}$$

Here m and e are, respectively, the mass and electric charge of an electron, k_B is the Boltzmann constant, and n_1 (n_2) denotes the number density of spin-up (spin-down) electrons, so that $n=n_1+n_2$. In the classical regime ($\Theta\gg1$), one may use the Coulomb coupling constant for such a classical system,[1]

$$\Gamma=\frac{e^2}{k_BT}\left[\frac{4\pi n}{3}\right]^{1/3}=2\left[\frac{4}{9\pi}\right]^{2/3}\frac{r_s}{\Theta} \tag{4}$$

in place of r_s.

Substantial progress has been achieved recently in the study of the correlational and thermodynamic properties for such an electron liquid.[2] The dielectric and thermodynamic functions have been calculated in the random-phase approximation[3–6] (RPA) or in the approaches[7,8] involving the local-field correction (LFC),[1,2] which describes the strong-coupling effects beyond the RPA. Accuracy of those calculations has been examined critically[1,2] through comparison with the Monte Carlo (MC) simulation results in the classical[9] as well as in the degenerate[10,11] limits. It has been well recognized[2] that the study of the strongly coupled charged liquids would yield crucial information for the understanding of such diverse physical systems as solid and fluid metals,[12,13] the molten alkali halides,[14] the inertial-confinement fusion experiments,[15] and interiors of various astrophysical objects.[16]

In this paper we aim at extending the line of theoretical studies mentioned above, and calculate the thermodynamic functions of the electron liquid in a self-consistent way over a wide range of the parametric combinations: r_s, Θ, and ζ. The computed results will be parametrized in the form of analytic formulas; the Fermi-liquid parameters are derived therefrom. We shall then investigate the density- and spin-response functions of the electron liquid and find that those functions change dramatically across the *phase boundary* curves on the n-T plane, associated with divergence to infinity of the isothermal compressibility and of the spin susceptibility. It will therefore be shown that the spin-dependent and phonon-induced electron interactions exhibit remarkable changes across the phase boundaries.[17] These findings may have significant consequences in electronic transport in metallic substances including superconductivity.

The problems described above are approached in this paper by a method of integral equations. In so doing we set a number of theoretical requirements: (i) Accuracy and self-consistency in predicting the thermodynamic functions over a wide range of the parameters: r_s, Θ, and ζ, (ii) simplicity in the structure of integral equations, and (iii) ability to describe the spin-dependent electron interactions. Requirement (ii), somewhat contradictory to (i), is needed because the integral equations are to be solved for *numerous* combinations of the three parameters in the derivation of the equation of state and in the construction of the phase diagram.

A theoretical scheme fulfilling those requirements may be provided by the spin-dependent density-response for-

malism, coupled with evaluation of the LFC's in what will be called the modified-convolution approximation (MCA). For the classical one-component plasma (OCP) or the electron liquid in the classical limit, it has been shown[18,19] that the MCA scheme offers a good compromise between simplicity in the structure of integral equations and accuracy in predicting the thermodynamic quantities self-consistently. It will be shown in this paper that the same statement applies also for the electron liquid in the degenerate limit. We thus expect that the MCA may likewise be applicable at intermediate degeneracies ($\Theta \simeq 1$) as an interpolation between those two limits, and hence over a wide range of parametric combinations.

In Sec. II we introduce the spin-dependent density-response formalism; the self-consistency conditions for the LFC's are taken up in Sec. III. The MCA scheme, that is, the approximation scheme used in this paper for the calculation of the spin-dependent LFC's, is described in Sec. IV. The set of integral equations in the MCA are solved for numerous combinations of r_s, Θ, and ζ; the results for the correlation functions are presented and examined in Sec. V. The thermodynamic functions are derived and discussed in Secs. VI and VII; the Fermi-liquid parameters are calculated therefrom in Sec. VIII. The thermodynamic instabilities associated with the compressibility and spin-susceptibility anomalies are discussed in Sec. IX, where the associated phase boundary curves are drawn on the n-T plane. The features of the spin-dependent and phonon-induced electron interactions are investigated in Sec. X. Concluding remarks are given in Sec. XI.

II. DENSITY-RESPONSE FORMALISM

To probe the correlational properties between the electrons,[1,2,12] we begin by applying to the system a weak, frequency ω and wave vector $\mathbf{k}$ dependent, external potential field $V_\sigma^{\rm ext}(\mathbf{k},\omega)$ which couples only to the density field on the spin component σ ($=1,2$). The induced density fluctuations $\delta n_\sigma(\mathbf{k},\omega)$ are then expressed as

$$\delta n_\sigma(\mathbf{k},\omega)=\sum_\tau \chi_{\sigma\tau}(k,\omega)V_\tau^{\rm ext}(\mathbf{k},\omega)\ . \tag{5}$$

These relations define the density-density response functions $\chi_{\sigma\tau}(k,\omega)$ between the spin components σ and τ.

In the polarization-potential approach[20] or the static LFC approximation,[2,12] the induced density fluctuations may be written as[21–23]

$$\delta n_\sigma(\mathbf{k},\omega)=\chi_\sigma^{(0)}(k,\omega)\times\left[V_\sigma^{\rm ext}(\mathbf{k},\omega)+\sum_\tau v(k)[1-G_{\sigma\tau}(k)]\delta n_\tau(\mathbf{k},\omega)\right]\ . \tag{6}$$

Here $v(k)=4\pi e^2/k^2$ is the bare Coulomb potential and $\chi_\sigma^{(0)}(k,\omega)$ are the free-particle polarizabilities; $G_{\sigma\tau}(k)$ are the spin-dependent LFC's.[2,12]

Comparison between Eqs. (5) and (6) yields explicit expressions for $\chi_{\sigma\tau}(k,\omega)$ in terms of $\chi_\sigma^{(0)}(k,\omega)$ and $G_{\sigma\tau}(k)$. The resulting forms are the same as those obtained earlier for multicomponent plasmas [see, e.g., Eqs. (17) and (18) in Ref. 23]. The static structure factors $S_{\sigma\tau}(k)$ and the pair distribution functions $g_{\sigma\tau}(r)$ are then calculated with the aid of the fluctuation-dissipation theorem, as formulated in detail in Ref. 2.

The density- and spin-response functions, $\chi(k,\omega)$ and $\chi_-(k,\omega)$, are calculated as

$$\chi(k,\omega)=\sum_\sigma\sum_\tau \chi_{\sigma\tau}(k,\omega)\ , \tag{7}$$

$$\chi_-(k,\omega)=\sum_\sigma\sum_\tau (2\delta_{\sigma\tau}-1)\chi_{\sigma\tau}(k,\omega)\ . \tag{8}$$

The density (charge) and spin parts of other correlation and response functions are defined analogously.[2,12,24,25]

In the paramagnetic limit ($\zeta=0$), the correlation and response functions depend only on the relative orientation of the spins. The correlation and response functions between electrons with parallel and antiparallel spins are then denoted by the suffixes p and a, respectively.

III. SELF-CONSISTENCY CONDITIONS

Once explicit expressions for $G_{\sigma\tau}(k)$ are obtained, the formalism described in the preceding section leads to a set of self-consistent integral equations for the correlations, which may be solved numerically by iteration. The expressions for $G_{\sigma\tau}(k)$ themselves have to satisfy a number of exact boundary conditions derived from short-range asymptotic behaviors and thermodynamic self-consistency requirements. In this section we summarize those conditions for the spin-polarized electron liquids.

We first note a self-consistency condition for the short-range correlations,

$$\lim_{k\to\infty} G_{\sigma\tau}(k)=1-g_{\sigma\tau}(0)\ . \tag{9}$$

This condition may be derived with the aid of the short-range asymptotic expansions of $S_{\sigma\tau}(k)$, a general property[26] of the Fourier transform between $S_{\sigma\tau}(k)$ and $g_{\sigma\tau}(r)$, and the cusp condition[25,26] for $g_{\sigma\tau}(r)$.

The generalized compressibility sum rules,[27,28]

$$\lim_{k\to 0}[-v(k)G_{\sigma\tau}(k)]=\frac{\partial^2}{\partial n_\sigma\,\partial n_\tau}\left[\frac{F_{\rm xc}}{V}\right]\ , \tag{10}$$

set the thermodynamic self-consistency conditions. Here $F_{\rm xc}/V$ is the exchange-correlation free-energy density. In the paramagnetic limit, the usual compressibility and spin-susceptibility sum rules[25,27,29] are recovered. For a numerical examination, we introduce dimensionless quantities,

$$\gamma_0^{\rm LFC}=\lim_{k\to 0}\left[\left[\frac{k_F}{k}\right]^2 G(k)\right]\ , \tag{11a}$$

$$\gamma_0^{\rm EOS}=-\frac{k_F^2}{4\pi e^2}\frac{\partial^2}{\partial n^2}\left[\frac{F_{\rm xc}}{V}\right]\Bigg|_{\zeta=0}=-\frac{k_F^2}{4\pi e^2}\frac{1}{n^2\kappa_{\rm xc}}\ , \tag{11b}$$

$$\gamma_{-}^{\mathrm{LFC}}=\lim_{k\to 0}\left[\left(\frac{k_F}{k}\right)^2 G_{-}(k)\right], \tag{12a}$$

$$\gamma_{-}^{\mathrm{EOS}}=-\frac{k_F^2}{4\pi n^2 e^2}\frac{\partial^2}{\partial\zeta^2}\left[\frac{F_{\mathrm{xc}}}{V}\right]\Bigg|_{\zeta=0}=-\frac{k_F^2}{4\pi e^2}\frac{\alpha_{\mathrm{xc}}}{n}. \tag{12b}$$

Here κ_{xc} and α_{xc} are the exchange-correlation contributions to the isothermal compressibility[29] and the spin stiffness[11] in the paramagnetic state; $G(k)$ and $G_{-}(k)$ are the charge and spin LFC's[2,12,24,25] $k_F=(3\pi^2 n)^{1/3}$ is the Fermi wave number. The comparison between γ_0^{LFC} and γ_0^{EOS} measures the extent to which the isothermal compressibility sum rule is satisfied; the comparison between $\gamma_{-}^{\mathrm{LFC}}$ and $\gamma_{-}^{\mathrm{EOS}}$ likewise yields information about the spin-susceptibility sum rule.

IV. SPIN-DEPENDENT LOCAL-FIELD CORRECTIONS

Let us proceed to derive an approximation scheme for the calculation of the spin-dependent LFC's, $G_{\sigma\tau}(k)$. For this purpose, we start working with the density-fluctuation operators[30]

$$\rho_\sigma(\mathbf{k})=\sum_{j=1}^{N_\sigma}\exp(-i\mathbf{k}\cdot\mathbf{r}_{j\sigma}), \tag{13}$$

where $\mathbf{r}_{j\sigma}$ represents the spatial coordinate of the jth particle with spin σ and N_σ is the number of electrons with spin σ. The equation of motion for $\rho_\sigma(\mathbf{k})$ reads[30]

$$\frac{\partial^2}{\partial t^2}\rho_\sigma(\mathbf{k})=-\sum_{j=1}^{N_\sigma}\left[\frac{\mathbf{k}\cdot\mathbf{p}_{j\sigma}}{m}+\frac{\hbar k^2}{2m}\right]^2\exp(-i\mathbf{k}\cdot\mathbf{r}_{j\sigma})$$
$$-\frac{4\pi e^2}{mV}\sum_\tau\sum_{\mathbf{q}\,(\neq 0)}\frac{\mathbf{k}\cdot\mathbf{q}}{q^2}\rho_\sigma(\mathbf{k}-\mathbf{q})\rho_\tau(\mathbf{q}), \tag{14}$$

where $\mathbf{p}_{j\sigma}$ denotes the momentum of the jth particle with spin σ.

The last term of Eq. (14) stems from the Coulomb interaction between electrons; we remark here that the self-interaction terms, i.e., the products between the contributions from the same electron in ρ_σ and ρ_τ, should be omitted. In the light of Eq. (6), we may replace the Coulomb-interaction term by[18]

$$-\frac{4\pi e^2}{mV}\sum_\tau\sum_{\mathbf{q}\,(\neq 0)}\frac{\mathbf{k}\cdot\mathbf{q}}{q^2}\rho_\sigma(\mathbf{k}-\mathbf{q})\rho_\tau(\mathbf{q})$$
$$=-\frac{4\pi N_\sigma e^2}{mV}\sum_\tau[1-G_{\sigma\tau}(k)]\rho_\tau(\mathbf{k}),$$

so that

$$N_\sigma\sum_\tau G_{\sigma\tau}(k)\rho_\tau(\mathbf{k})=-\sum_\tau{\sum_{\mathbf{q}}}'\frac{\mathbf{k}\cdot\mathbf{q}}{q^2}\rho_\sigma(\mathbf{k}-\mathbf{q})\rho_\tau(\mathbf{q}), \tag{15}$$

where the prime means omission of the terms with $\mathbf{q}=\mathbf{0}$ and $\mathbf{q}=\mathbf{k}$ in the $\mathbf{q}$ summation. We multiply Eq. (15) by $\rho_\upsilon(-\mathbf{k})$ and carry out the statistical average denoted by $\langle\ \rangle$. We thus obtain

$$\sum_\tau\left[\frac{N_\tau}{N_\upsilon}\right]^{1/2}G_{\sigma\tau}(k)S_{\tau\upsilon}(k)=-\frac{1}{N_\sigma N_\upsilon}\sum_\tau{\sum_{\mathbf{q}}}'I(\mathbf{k},\mathbf{q})\left\langle\sum_{i=1}^{N_\sigma}\sum_{\substack{j=1\\(j\neq i)}}^{N_\tau}\sum_{l=1}^{N_\upsilon}\exp[-i(\mathbf{k}-\mathbf{q})\cdot\mathbf{r}_{i\sigma}]\exp(-i\mathbf{q}\cdot\mathbf{r}_{j\tau})\exp(i\mathbf{k}\cdot\mathbf{r}_{l\upsilon})\right\rangle \tag{16}$$

with

$$I(\mathbf{k},\mathbf{q})=\mathbf{k}\cdot\mathbf{q}/q^2. \tag{17}$$

We express the right-hand side of Eq. (16) in terms of the pair and ternary correlation functions,[31] $h_{\sigma\tau}(r)$ and $h_{\sigma\tau\upsilon}(\mathbf{r}_1,\mathbf{r}_2,\mathbf{r}_3)$. We then introduce the *convolution approximation*,[1,32] so that the ternary correlation functions are expressed as

$$h_{\sigma\tau\upsilon}(\mathbf{r}_1,\mathbf{r}_2,\mathbf{r}_3)=h_{\sigma\tau}(r_{12})h_{\tau\upsilon}(r_{23})+h_{\tau\upsilon}(r_{23})h_{\upsilon\sigma}(r_{31})+h_{\upsilon\sigma}(r_{31})h_{\sigma\tau}(r_{12})+\sum_\mu n_\mu\int d\mathbf{r}_4\,h_{\sigma\mu}(r_{14})h_{\tau\mu}(r_{24})h_{\upsilon\mu}(r_{34}). \tag{18}$$

The approximation (18) satisfies the sequential relations[2,33] between the pair and ternary correlation functions; it has been recognized[2,33] essential to maintain the sequential relations especially for the long-ranged Coulomb system. Substitution of Eq. (18) in Eq. (16) yields

$$\sum_\tau\left[\frac{N_\tau}{N_\upsilon}\right]^{1/2}G_{\sigma\tau}(k)S_{\tau\upsilon}(k)=-\frac{1}{N_\sigma N_\upsilon}\sum_\tau{\sum_{\mathbf{q}}}'I(\mathbf{k},\mathbf{q})\left[\sum_\mu\left[\frac{N_\sigma N_\tau N_\upsilon}{N_\mu}\right]^{1/2}S_{\sigma\mu}(\mathbf{k}-\mathbf{q})S_{\tau\mu}(q)S_{\upsilon\mu}(k)\right.$$
$$\left.-\delta_{\sigma\tau}(N_\tau N_\upsilon)^{1/2}S_{\tau\mu}(k)\right]. \tag{19}$$

Generally the solution of Eq. (19) does not satisfy the symmetry relations $G_{\sigma\tau}(k)=G_{\tau\sigma}(k)$ because the symmetry with respect to interchange of the indices has been broken by the introduction of the convolution approximation, Eq. (18). Symmetrization is thus carried out between σ and τ, and so we find

$$G_{11}(k)=-\frac{1}{n_1}\int\frac{d\mathbf{q}}{(2\pi)^3}\left\{\left[K(\mathbf{k},\mathbf{q})R_{11}(q)+\left[\frac{n_2}{n_1}\right]^{1/2}I(\mathbf{k},\mathbf{q})R_{12}(q)\right][S_{11}(\mathbf{k}-\mathbf{q})-1]+\left[\frac{n_2}{n_1}\right]^{1/2}J(\mathbf{k},\mathbf{q})R_{11}(q)S_{12}(\mathbf{k}-\mathbf{q})\right\}, \tag{20a}$$

$$G_{12}(k)=-\frac{1}{2(n_1n_2)^{1/2}}\int\frac{d\mathbf{q}}{(2\pi)^3}\left\{\left\{\left[\left[\frac{n_2}{n_1}\right]^{1/2}+\left[\frac{n_1}{n_2}\right]^{1/2}\right]K(\mathbf{k},\mathbf{q})R_{12}(q)+I(\mathbf{k},\mathbf{q})[R_{11}(q)+R_{22}(q)]\right\}S_{12}(\mathbf{k}-\mathbf{q})+J(\mathbf{k},\mathbf{q})R_{12}(q)[S_{11}(\mathbf{k}-\mathbf{q})-1]+J(\mathbf{k},\mathbf{q})R_{12}(q)[S_{22}(\mathbf{k}-\mathbf{q})-1]\right\}, \tag{20b}$$

with

$$J(\mathbf{k},\mathbf{q})=\mathbf{k}\cdot(\mathbf{k}-\mathbf{q})/|\mathbf{k}-\mathbf{q}|^2\ , \tag{21}$$

$$K(\mathbf{k},\mathbf{q})=I(\mathbf{k},\mathbf{q})+J(\mathbf{k},\mathbf{q})\ . \tag{22}$$

$G_{22}(k)$ may be obtained by interchanges of $1\leftrightarrow2$ in Eq. (20a). In Eqs. (20), $R_{\sigma\tau}(k)$ are given by

$$R_{\sigma\tau}(k)=\tfrac{1}{2}[\delta_{\sigma\tau}+S_{\sigma\tau}(k)] \tag{23}$$

and play the part of the screening functions.[18,19]

We remark at this stage that the approximation scheme proposed by Singwi, Tosi, Land, and Sjölander[34] (STLS) may be obtained in the present formalism by setting $S_{\sigma\tau}(k)=\delta_{\sigma\tau}$ in Eq. (23) or $R_{\sigma\tau}(k)=\delta_{\sigma\tau}$ in Eqs. (20). Departure of Eq. (23) from $\delta_{\sigma\tau}$ is substantial in the long-wavelength regime; the STLS scheme thus has an intrinsic difficulty in satisfying the generalized compressibility sum rules, Eqs. (10). For an OCP, the extent of this difficulty has been numerically investigated both in the classical[18,19] and degenerate[35] limits.

In the present theory we *modify* the convolution-approximation results and thereby simplify the calculations of $G_{\sigma\tau}(k)$ through a replacement of Eq. (23) by

$$R_{\sigma\tau}(k)=\tfrac{1}{2}[\delta_{\sigma\tau}+\bar{S}_{\sigma\tau}(k)]\ , \tag{24}$$

where the structure factors $\bar{S}_{\sigma\tau}(k)$ are parametrized as

$$\bar{S}(k)=k^2/(k^2+k_0^2)\ , \tag{25a}$$

$$\bar{S}_{11}(k)=(k^2+k_1^2)/(k^2+k_{01}^2)\ , \tag{25b}$$

$$\bar{S}_{12}(k)=\frac{n\bar{S}(k)-n_1\bar{S}_{11}(k)-n_2\bar{S}_{22}(k)}{2(n_1n_2)^{1/2}}\ , \tag{25c}$$

and $\bar{S}_{22}(k)$ is again given by interchanges of $1\leftrightarrow2$ in Eq. (25b). The characteristic wave numbers, k_0, k_1, k_{01}, k_2, and k_{02}, are determined from the self-consistency conditions:

$$\int\frac{d\mathbf{k}}{(2\pi)^3}v(k)[\bar{S}_{\sigma\tau}(k)-\delta_{\sigma\tau}]=\int\frac{d\mathbf{k}}{(2\pi)^3}v(k)[S_{\sigma\tau}(k)-\delta_{\sigma\tau}]\ , \tag{26a}$$

$$\bar{S}_{\sigma\tau}(0)=S_{\sigma\tau}(0)\ , \tag{26b}$$

where $S(k)$ and $S_{\sigma\tau}(k)$ refer to the solutions to the integral equations. We thus obtain a closed set of integral equations for $S_{\sigma\tau}(k)$ and $G_{\sigma\tau}(k)$. As we will soon demonstrate, the screening effects introduced through Eqs. (24)–(26) play a vital role in accounting for the correlation properties of the strongly coupled electron liquids in the long-wavelength regime. We shall call the resulting evaluations of $G_{\sigma\tau}(k)$ the MCA scheme.

For a paramagnetic electron liquid, Eqs. (20) lead to

$$G(k)=-\frac{1}{n}\int\frac{d\mathbf{q}}{(2\pi)^3}K(\mathbf{k},\mathbf{q})R(q)[S(\mathbf{k}-\mathbf{q})-1]\ , \tag{27a}$$

$$G_-(k)=-\frac{1}{n}\int\frac{d\mathbf{q}}{(2\pi)^3}\{I(\mathbf{k},\mathbf{q})R(q)[S_-(\mathbf{k}-\mathbf{q})-1]+J(\mathbf{k},\mathbf{q})R_-(q)[S(\mathbf{k}-\mathbf{q})-1]\}\ . \tag{27b}$$

Here $S(k)$ and $S_-(k)$ are the charge and spin structure factors and we define

$$R(k)=[1+\bar{S}_p(k)+\bar{S}_a(k)]/2=[1+\bar{S}(k)]/2\ , \tag{28a}$$

$$R_-(k)=[1+\bar{S}_p(k)-\bar{S}_a(k)]/2=[1+\bar{S}_-(k)]/2\ . \tag{28b}$$

In the ferromagnetic limit, we analogously find

$$G_{11}(k)=-\frac{1}{n_1}\int\frac{d\mathbf{q}}{(2\pi)^3}K(\mathbf{k},\mathbf{q})R_{11}(q)[S_{11}(\mathbf{k}-\mathbf{q})-1]\ . \tag{29}$$

V. CORRELATION FUNCTIONS

We solve the MCA integral equations numerically for $S_{\sigma\tau}(k)$ and $G_{\sigma\tau}(k)$ at various parametric combinations: $\Theta=0$, 0.05, 0.1, 0.2, 0.5, 1, 2, and 5; $0\le r_s\le175$; $\zeta=0$, 0.2, 0.5, 0.8, and 1. For comparison, we also solve the STLS integral equations[24,34] newly for $r_s\le100$ in the paramagnetic ($\zeta=0$) and ferromagnetic ($\zeta=1$) states at $\Theta=0$. The computational procedure is analogous to that in Ref. 7.

In the calculations of the LFC's, Eqs. (20) and (24), the angular integration between $\mathbf{k}$ and $\mathbf{k}-\mathbf{q}$ can be carried out analytically, so that the LFC's are expressed in terms of the integrations over a single variable. The computational time needed to solve the integral equations in the

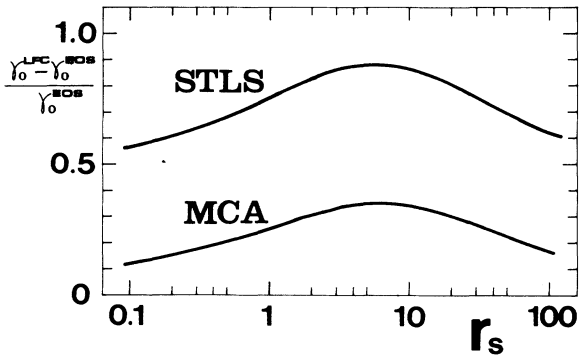

FIG. 1. The difference of the compressibility coefficient γ_0 between the estimations through the local-field correction (LFC) and the equation of state (EOS) in the paramagnetic ($\zeta=0$) state at $\Theta=0$. MCA and STLS refer to the calculations of $\gamma_0^{\rm LFC}$ on the basis of the modified-convolution approximation and of the Singwi-Tosi-Land-Sjölander approximation (Ref. 34). The values of $\gamma_0^{\rm EOS}$ are calculated from the fitting formula by Vosko, Wilk, and Nusair (Ref. 11).

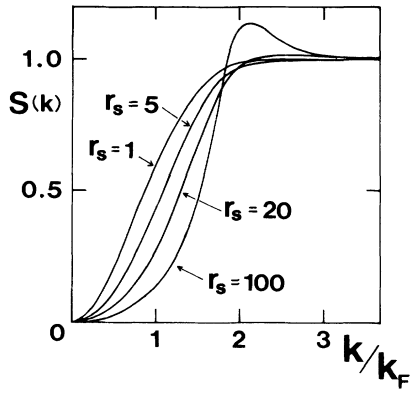

FIG. 3. Charge structure factor for $r_s=1$, 5, 20, and 100 at $\Theta=0$ and $\zeta=0$. $k_F=(3\pi^2 n)^{1/3}$ is the Fermi wave number in the paramagnetic state.

MCA scheme is therefore of the same order as that in the STLS scheme. Such simplicity is valuable particularly when iterative solutions to the integral equations are to be obtained over numerous combinations of the plasma parameters.

On the basis of those numerical results, let us investigate the self-consistency conditions mentioned in Sec. III: To begin, we remark that the expressions for $G_{\sigma\tau}(k)$ as given by Eqs. (20) satisfy the short-range conditions (9) exactly.

As for the compressibility sum rule, we show in Fig. 1 the computed results of $(\gamma_0^{\rm LFC}-\gamma_0^{\rm EOS})/\gamma_0^{\rm EOS}$ in the paramagnetic ($\zeta=0$) ground state ($\Theta=0$) as functions of r_s, both in the MCA scheme and in the STLS scheme. The equation of state used here for the calculation of $\gamma_0^{\rm EOS}$ is that obtained in the Green's-function Monte Carlo (GFMC) calculations.[10,11] The equation of state obtained either in the MCA scheme or in the STLS scheme, however, leads to a prediction of $\gamma_0^{\rm EOS}$ almost identical to the GFMC value. Apparently in Fig. 1 the MCA values of $\gamma_0^{\rm LFC}$ improve significantly over the STLS values.

We have similarly examined the compressibility sum rule in the ferromagnetic ($\zeta=1$) state at $\Theta=0$ and observed an analogous improvement in the MCA result over the STLS result.

We compare in Fig. 2 the result for the spin-susceptibility sum rule between the MCA and STLS calculations at $\Theta=0$ and $\zeta=0$. Again we observe a significant improvement in the MCA values as compared with the STLS values.

The numerical results in the MCA scheme for $S(k)$, $g(r)$, $G(k)$, and $G_-(k)$ are plotted in Figs. 3–6 for various values of r_s at the paramagnetic ($\zeta=0$) ground state ($\Theta=0$). As examined above, the MCA scheme accurately describes the long-range correlations in the degenerate electron liquid as well as in the classical OCP.[19] On the other hand, the MCA scheme has a defect in that $g(r)$ becomes negative in the vicinity of the origin for $r_s \gtrsim 5$, as observed in Fig. 4; this is the cost that one has to pay in

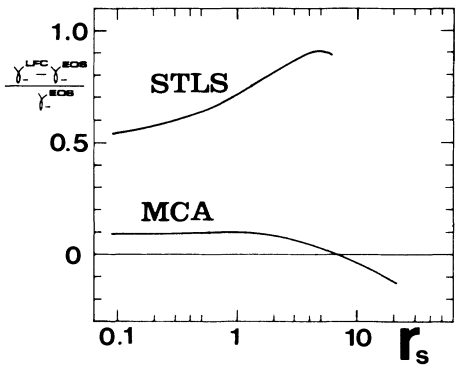

FIG. 2. The difference of the spin-susceptibility coefficient γ_- between the estimations through the local-field correction and the equation of state in the paramagnetic ($\zeta=0$) state at $\Theta=0$. Otherwise the same as in Fig. 1.

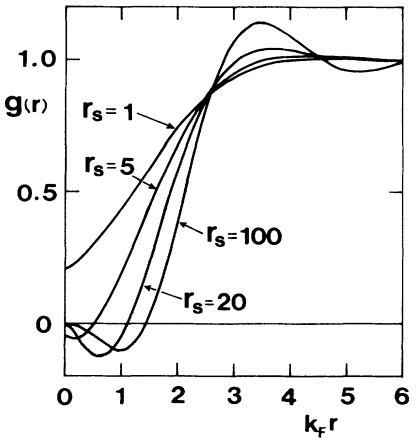

FIG. 4. Pair distribution function for various values of r_s at $\Theta=0$ and $\zeta=0$.

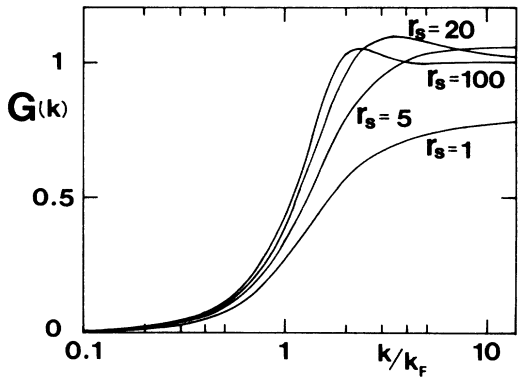

FIG. 5. Charge local-field correction $G(k)$ at $\Theta=0$ and $\zeta=0$.

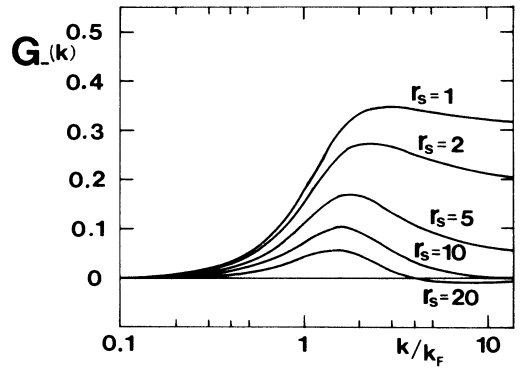

FIG. 6. Spin local-field correction $G_{-}(k)$ at $\Theta=0$ and $\zeta=0$.

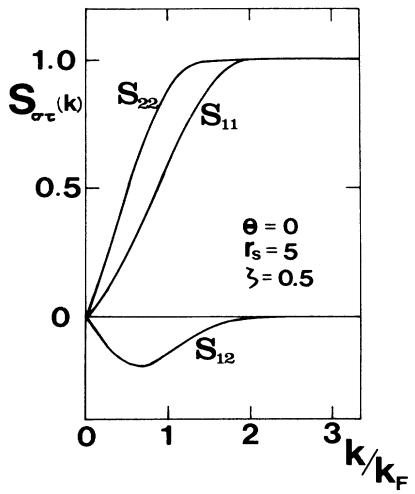

FIG. 7. Spin-dependent structure factors at $\Theta=0$, $r_s=5$, and $\zeta=0.5$. $k_F=(6\pi^2 n_1)^{1/3}$ is the Fermi wave number of the spin-up electrons.

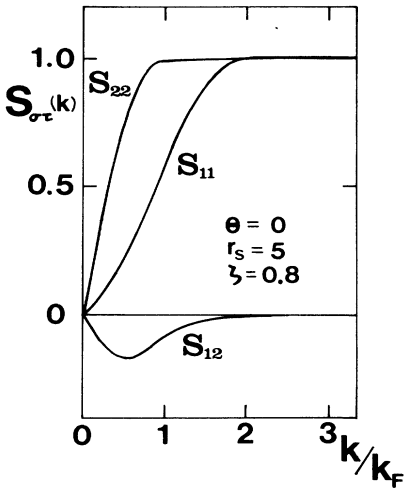

FIG. 8. Spin-dependent structure factors at $\Theta=0$, $r_s=5$, and $\zeta=0.8$.

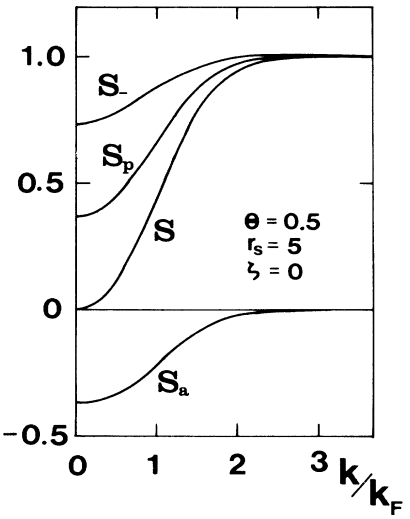

FIG. 9. Spin-dependent structure factors at $\Theta=0.5$, $r_s=5$, and $\zeta=0$.

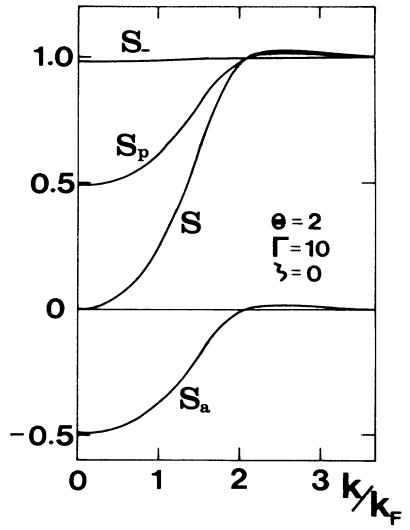

FIG. 10. Spin-dependent structure factors at $\Theta=2$, $\Gamma=10$, and $\zeta=0$.

the adopting of a simplified set of integral equations, aiming at an accuracy in the thermodynamic descriptions. In the case of a classical OCP, it has been shown[19] that due to such negativeness of $g(r)$ that causes an oscillation to $g(r)$ in the short-range region the overall shape of $g(r)$ becomes analogous to the MC result.[9]

To see how the structure factors depends on the spin polarization and Fermi degeneracy, we exhibit in Figs. 7–10 the computed values of $S_{\sigma\tau}(k)$ in the MCA scheme for some combinations of Θ, r_s (or Γ), and ζ. We observe in Figs. 9 and 10 that the spin-fluctuation structure factor $S_{-}(k)$ quickly approaches unity as the system enters the classical regime ($\Theta > 1$).

VI. THERMODYNAMIC FUNCTIONS

The Helmholtz free energy F of the system may be divided into two parts, i.e., the ideal part F_0 and the exchange-correlation part $F_{\rm xc}$ as

$$F = F_0 + F_{\rm xc} \ . \tag{30}$$

The ideal part can be calculated in the usual way.[36]

The exchange-correlation (or excess) free energy $F_{\rm xc}$ asymptotically approaches the lowest-order exchange (Hartree-Fock) free energy F_x in the weak-coupling limit ($r_s \to 0$ or $\Gamma \to 0$). The exchange part F_x is given by[6]

$$F_x = \sum_\sigma F_{x\sigma} \tag{31}$$

and

$$F_{x\sigma}/N_\sigma k_{F\sigma} e^2 = -(4/9\pi)^{1/3} a(\Theta_\sigma) \ . \tag{32}$$

Here $k_{F\sigma} = (6\pi^2 n_\sigma)^{1/3}$ and $a(\Theta_\sigma)$ is an exchange integral[7] with the reduced temperature Θ_σ. An accurate fitting formula for $a(\Theta_\sigma)$ has been derived by Perrot and Dharma-wardana[5] [see Eq. (42) and Table V].

We have calculated the interaction energy $E_{\rm int}$ in the MCA scheme for 683 combinations of the plasma parameters in the range of $\Theta = 0$, 0.05, 0.1, 0.2, 0.5, 1, 2, and 5, $0 \le r_s \le 175$, and $\zeta = 0$, 0.2, 0.5, 0.8, and 1. The excess free energy is then calculated through[29,36]

$$f_{\rm xc}(c,\Theta,\zeta) = \frac{1}{c}\int_0^c dx\ \varepsilon_{\rm int}(x,\Theta,\zeta) \ , \tag{33}$$

where $f_{\rm xc} = F_{\rm xc}/N(e^2/a)$, $\varepsilon_{\rm int} = E_{\rm int}/N(e^2/a)$, $a = (4\pi n/3)^{-1/3}$, and $c = r_s$ or Γ (i.e., the dimensionless coupling constant). Finally the correlation free energy F_c is given by

$$F_c = F_{\rm xc} - F_x \ . \tag{34}$$

We have performed explicit calculation of $f_{\rm xc}$ in the following way: For $\zeta = 0$ and 1, the coupling-constant integration of Eq. (33) is carried out numerically with the aid of the cubic-spline-polynomial interpolation. Such a procedure is not applicable to the cases of $0 < \zeta < 1$ since the computed values exist sparsely. Here we instead assume a ζ dependence of $\varepsilon_{\rm int}$ as

$$\varepsilon_{\rm int}(c,\Theta,\zeta) = \varepsilon_{\rm int}(c,\Theta,0) + \tfrac{1}{2}s(c,\Theta)\zeta^2 + t(c,\Theta)\zeta^4 + u(c,\Theta)\zeta^6 \ . \tag{35}$$

We then set

$$t(c,\Theta) = \tfrac{5}{108}s(c,\Theta) \ , \tag{36}$$

adopting the relation found in the Hartree-Fock approximation at $\Theta = 0$. We have checked that the relation (36) is satisfied with a good accuracy also in the RPA calculation[11] at $\Theta = 0$. The coefficient u is then determined so that Eq. (35) reproduces the computed values in the ferromagnetic limit ($\zeta \to 1$). We thus find

$$\varepsilon_{\rm int}(c,\Theta,\zeta) = (1-\zeta^6)\varepsilon_{\rm int}(c,\Theta,0) + \zeta^6\varepsilon_{\rm int}(c,\Theta,1) + (\tfrac{1}{2}\zeta^2 + \tfrac{5}{108}\zeta^4 - \tfrac{59}{108}\zeta^6)s(c,\Theta) \ , \tag{37}$$

whence

$$f_{\rm xc}(c,\Theta,\zeta) = (1-\zeta^6)f_{\rm xc}(c,\Theta,0) + \zeta^6 f_{\rm xc}(c,\Theta,1) + (\tfrac{1}{2}\zeta^2 + \tfrac{5}{108}\zeta^4 - \tfrac{59}{108}\zeta^6)\frac{\alpha_{\rm xc}}{e^2/a} \tag{38}$$

with

$$\frac{\alpha_{\rm xc}}{e^2/a} = \frac{1}{c}\int_0^c dx\ s(x,\Theta) \ . \tag{39}$$

The coefficient s may be evaluated by using the values of $\varepsilon_{\rm int}$ at $\zeta = 0.2$ at fixed values of r_s and Θ. The computed values of $\varepsilon_{\rm int}(\zeta) - \varepsilon_{\rm int}(0)$ at $\zeta = 0.5$ and 0.8 can then be reproduced by Eq. (37) with the digressions of less than 3% for all the cases computed. The interpolation formula (37) thus reproduces the computed values at the intermediate spin polarizations with an accuracy much superior to the von Barth–Hedin type interpolation[37] and with an accuracy comparable to the Vosko-Wilk-Nusair type interpolation.[11] We have fitted $s(c,\Theta)$ as a function of the coupling constant c for each Θ and carried out the in-

TABLE I. Ground-state energy in the paramagnetic state. MCA refers to the present calculation; STLS, the calculation based on the integral equations of Singwi *et al.* (Ref. 34); VMC, the variational Monte Carlo result (Ref. 38); GFMC, the Green's-function Monte Carlo result (Ref. 10). The energy is measured in units of mRy.

r_s	MCA	STLS	VMC	GFMC
1	1167	1171	1172	1174
2	−0.3	3.5	6.9	4.1
3	−138.2	−134.6	−132.1	
4	−158.2	−155.0	−153.3	
5	−154.4	−151.2	−149.9	−151.2
6	−144.8	−141.8		
10	−108.36	−105.86	−105.70	−106.75
15	−80.69	−78.57	−78.86	
20	−64.18	−62.33	−62.80	−63.29
30	−45.62	−44.14	−44.77	
50	−29.06	−27.97	−28.58	−28.84
75	−20.071	−19.249	−19.783	
100	−15.365	−14.699	−15.185	−15.321

TABLE II. Ground-state energy in the ferromagnetic state. Otherwise the same as Table I.

r_s	MCA	STLS	VMC	GFMC
1	2281	2285		
2	244.3	248.3		251.7
3	−41.6	−37.9		
4	−109.9	−106.4		
5	−126.7	−123.4		−121.4
6	−127.7	−124.6		
10	−104.6	−102.0	−101.3	−101.3
15	−79.99	−77.81		
20	−64.21	−62.33		−62.51
30	−45.93	−44.42	−44.7	
50	−29.31	−28.21	−28.73	−28.78
75	−20.237	−19.411		
100	−15.480	−14.812	−15.261	−15.340

TABLE III. Values of $-f_{xc} \equiv -F_{xc}/N(e^2/a)$ calculated in the MCA scheme for the paramagnetic (P) and ferromagnetic (F) states at $\Theta=0.2$ and 0.5.

	$\Theta=0.2$		$\Theta=0.5$	
r_s	P	F	P	F
1	0.512 23	0.603 94	0.471 15	0.561 20
2	0.548 60	0.626 68	0.522 07	0.596 53
3	0.574 15	0.643 08	0.556 15	0.620 56
4	0.592 66	0.655 32		
5	0.607 39	0.665 23	0.596 86	0.650 06
6	0.619 61	0.673 57		
10	0.654 12	0.697 58	0.651 42	0.690 49
20	0.699 12	0.729 96	0.700 10	0.727 50
30	0.723 16	0.747 77	0.725 11	0.746 88
50	0.750 17	0.768 26	0.752 48	0.768 45
75	0.768 78	0.782 71	0.770 98	0.783 27
100	0.780 46	0.791 93	0.782 46	0.792 60

tegration of Eq. (39) analytically to obtain the spin stiffness α_{xc}.

We list in Tables I and II the values of the ground-state energy computed in the MCA and STLS schemes and compare them with the variational Monte Carlo (VMC) result[38] and the GFMC result[10] in the paramagnetic and ferromagnetic states.

The spin-polarization dependence of the correlation energy E_c at the ground state is typically illustrated in Fig. 11, where the increment $\Delta E_c = E_c(\zeta) - E_c(0)$ is plotted as a function of ζ at $r_s = 5$. We observe in the figure that the RPA results[11] for ΔE_c resemble the MCA results closely although the values of E_c themselves are quite different from each other. The values of ΔE_c computed by Dunaevskii,[39] who used the LFC in the paramagnetic state parametrized by Singwi, Sjölander, Tosi, and Land[40] without regard to the spin polarization, show systematic deviations from the MCA and RPA results as ζ increases.

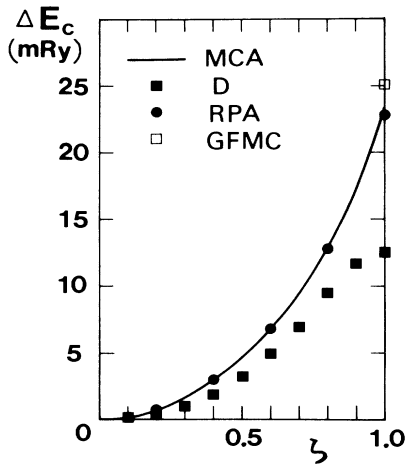

FIG. 11. Variations of $\Delta E_c = E_c(\zeta) - E_c(0)$ at $\Theta=0$ and $r_s=5$. MCA refers to the present calculation; GFMC, the calculation based on the Green's-function Monte Carlo method (Ref. 10); RPA, the random-phase approximation (Ref. 11); D, Dunaevskii (Ref. 39).

The values of the excess free energy f_{xc} in the paramagnetic and ferromagnetic states at finite temperatures are listed in Tables III and IV for typical values of Θ and r_s (or Γ). We recall that the MCA scheme has reproduced the MC values[9] of E_{int} within relative errors of 2% in the fluid phase of the classical OCP, as was shown in Ref. 19. We also remark that the MCA scheme reproduces the GFMC values[10,11] of E_{int} for $r_s \leq 100$ with digressions of less than 2% in the paramagnetic state and 3% in the ferromagnetic state at $\Theta=0$ (see Tables I and II). We thus expect that the values of f_{xc} listed in Tables III and IV may represent accurate (say, within relative errors of 5%) estimates of the exact excess free energies at finite temperatures as an interpolation between the classical and degenerate limits.

VII. PARAMETRIZED EXPRESSIONS FOR EQUATIONS OF STATE

We have parametrized the values of the interaction energy E_{int} computed in the MCA scheme in accord with

TABLE IV. Values of $-f_{xc}$ at $\Theta=1$ and 2.

	$\Theta=1$		$\Theta=2$	
Γ	P	F	P	F
0.5	0.392 43	0.474 17	0.369 38	0.422 00
1	0.456 54	0.524 76	0.447 39	0.490 75
2	0.524 74	0.579 36	0.527 48	0.561 55
3	0.568 71	0.614 76	0.577 93	0.606 21
5	0.618 59	0.655 38	0.632 84	0.654 99
8	0.660 56	0.689 81	0.677 43	0.694 71
10	0.678 89	0.704 92	0.696 46	0.711 69
15	0.709 22	0.730 01	0.727 33	0.739 30
20	0.728 34	0.745 90	0.746 36	0.756 36
30	0.751 90	0.756 59	0.769 31	0.776 98
40	0.766 37	0.777 74		
60	0.776 40	0.786 21		

Eq. (37). The result is expressed as

$$\varepsilon_{\rm int}(r_s,\Theta,i)=-\frac{a_i(\Theta)+b_i(\Theta)r_s^{1/2}+c_i(\Theta)r_s}{1+d_i(\Theta)r_s^{1/2}+e_i(\Theta)r_s} \quad (i=0,1)\ , \tag{40}$$

$$s(r_s,\Theta)=-\frac{a_s(\Theta)+b_s(\Theta)r_s}{1+c_s(\Theta)r_s+d_s(\Theta)r_s^2}\ . \tag{41}$$

The coefficients $a-e$ in Eqs. (40) and (41) are parametrized as functions of Θ in a universal form as

$$f(\Theta)=F(\Theta)\frac{1+x_2\Theta^2+x_3\Theta^3+x_4\Theta^4}{1+y_2\Theta^2+y_3\Theta^3+x_y\Theta^4}\ . \tag{42}$$

The values of x_j and y_j ($j=2,3,4$) and the functional forms of $F(\Theta)$ and tabulated in Table V. Assuming the functional forms of $\varepsilon_{\rm int}$ and s in Eqs. (40) and (41), we first determine the values of $a-e$ at fixed Θ and then fix the coefficients in the functions $a-e$. Those fitting formulas reproduce the computed values of $E_{\rm int}$ for all the 683 cases with relative errors less than 1.5%.

Formulas (40)–(42) have been constructed so as to reproduce accurately the known results in the classical limit.[1,9,41] In the weak-coupling limit, they reduce to the Debye-Hückel form,[1,31] and agree with the numerical values[41] obtained through solution to the hypernetted chain equation[1,2] within 0.1% for $\Gamma\le 1$. In the strong-coupling regime, formulas (40)–(42) reproduce the MC values[9] for $1\le\Gamma\le 200$ with digressions of less than 0.5%, and likewise reproduce the GFMC values[10,11] for $r_s\le 100$ within relative errors of 3% in the degenerate limit. Assuming that the MCA scheme gives an appropriate interpolation of $E_{\rm int}$ as a function of Θ, r_s, and ζ, and taking account of the errors (1.5%) in constructing the fitting formulas, we may tentatively say that formulas (40)–(42) can give the "true" values of $E_{\rm int}$ within relative errors of approximately 5% over the whole region of the fluid phase.

The expression for the excess free energy $F_{\rm xc}$ is then obtained by performing the coupling-constant integration as prescribed by Eq. (33). The result is given by Eq. (38) with

$$\frac{\alpha_{\rm xc}}{N(e^2/a)}=-\frac{1}{r_s}\left[\frac{b_s}{2d_s}\ln|1+c_sr_s+d_sr_s^2| +\frac{2a_sd_s-b_sc_s}{2d_s(c_s^2-4d_s)^{1/2}}\left[\ln\left|\frac{2d_sr_s+c_s-(c_s^2-4d_s)^{1/2}}{2d_sr_s+c_s+(c_s^2-4d_s)^{1/2}}\right|-\ln\left|\frac{c_s-(c_s^2-4d_s)^{1/2}}{c_s+(c_s^2-4d_s)^{1/2}}\right|\right]\right]\ , \tag{43}$$

$$f_{\rm xc}(r_s,\Theta,0)=-\frac{c_0}{e_0}-\frac{2}{e_0}\left[b_0-\frac{c_0d_0}{e_0}\right]r_s^{-1/2}-\frac{1}{e_0r_s}\left[\left[a_0-\frac{c_0}{e_e}\right]-\frac{d_0}{e_0}\left[b_0-\frac{c_0d_0}{e_0}\right]\right]\ln|e_0r_s+d_0r_s^{1/2}+1| +\frac{2}{e_0(4e_0-d_0^2)^{1/2}r_s}\left[d_0\left[a_0-\frac{c_0}{e_0}\right]+\left[2-\frac{d_0^2}{e_0}\right]\left[b_0-\frac{c_0d_0}{e_0}\right]\right] \times\left[\tan^{-1}\left[\frac{2e_0r_s^{1/2}+d_0}{(4e_0-d_0^2)^{1/2}}\right]-\tan^{-1}\left[\frac{d_0}{(4e_0-d_0^2)^{1/2}}\right]\right]\ , \tag{44}$$

TABLE V. Values of x_j and y_j ($j=2,3,4$) and functional forms of $F(\Theta)$ in Eq. (42) for the coefficients $a-e$ appearing in Eqs. (40) and (41). The symbol "-" means that the corresponding terms have not been adopted in the approximants.

$f(\Theta)$	$F(\Theta)$	x_2	x_3	x_4	y_2	y_3	y_4
$a_0(\Theta)$	$0.458\,165\tanh(1/\Theta)$	4.058 17	−0.123 027	2.271 33	8.310 51	-	5.1105
$b_0(\Theta)$	$0.536\,660 d_0(\Theta)$	13.0190	2.843 94	-	8.100 97	2.147 76	-
$c_0(\Theta)$	$0.866\,914 e_0(\Theta)$	0.983 008	0.431 746	-	1.044 74	0.416 920	-
$d_0(\Theta)$	$0.511\,152\tanh(1/\Theta^{1/2})$	11.1117	126.789	1.756 92	1.0	75.0184	1.0
$e_0(\Theta)$	$0.373\,518\tanh(1/\Theta)$	0.798 047	0.193 051	1.773 36	1.0	1.030 64	1.0
$a_1(\Theta)$	$1.259\,92 a_0(0.629\,961\Theta)$	-	-	-	-	-	-
$b_1(\Theta)$	$0.603\,045 d_1(\Theta)$	5.088 61	1.850 33	-	3.233 86	1.570 23	-
$c_1(\Theta)$	$0.865\,647 e_1(\Theta)$	0.749 519	0.499 229	-	0.818 992	0.481 380	-
$d_1(\Theta)$	$0.508\,784\tanh(1/\Theta^{1/2})$	4.797 54	133.956	1.765 09	1.0	76.7183	1.0
$e_1(\Theta)$	$0.311\,335\tanh(1/\Theta)$	1.446 45	−1.666 39	2.127 55	1.0	0.119 757	1.0
$a_s(\Theta)$	0.203 629	3.531 90	2.0	-	0.674 757	2.201 26	1.0
$b_s(\Theta)$	0.215 506	41.2764	-	-	4.402 26	-	12.7681
$c_s(\Theta)$	1.722 62	36.0644	-	-	5.463 83	-	5.564 74
$d_s(\Theta)$	0.282 782	41.2038	-	-	2.133 88	-	9.375 39

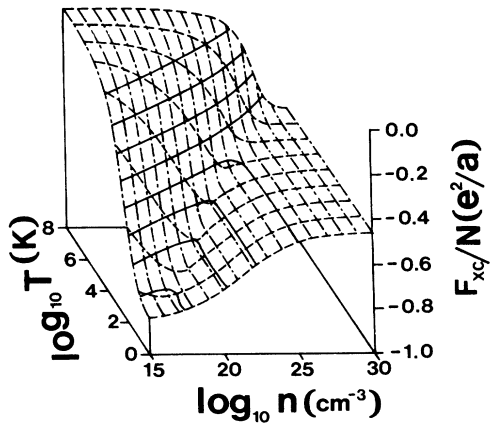

FIG. 12. Reduced excess free energy $f_{xc}=F_{xc}/N(e^2/a)$ in the paramagnetic state for 10^{15} cm$^{-3}\leq n\leq 10^{30}$ cm^{-3} and $1K\leq T\leq 10^8$ K. Three types of contours are depicted: $n=$const (dot-dashed curves); $T=$const (dashed curves); $f_{xc}=$const (solid curves).

and an analogous expression for $f_{xc}(c,\Theta,1)$.

The numerical values derived from those analytic expressions behave smoothly over the whole region in the fluid phase of the electron OCP. We plot in Figs. 12 and 13 the behaviors of $f_{xc}(r_s,\Theta,0)$ and $f_{xc}(r_s,\Theta,1)$ calculated from the fitting formulas as functions of the number density n and the temperature T for $10^{15}\leq n\leq 10^{30}$ cm^{-3} and $1\leq T\leq 10^8$ K.

VIII. FERMI-LIQUID PARAMETERS

In this section we calculate the Fermi-liquid parameters of the electron fluids such as the effective mass, the spin susceptibility, and the isothermal compressibility, on the basis of the values of E_{int} and F_{xc} calculated in the preceding sections.

The effective mass m_σ^* is related to the specific heat C_V via[29,42]

$$C_V=-T\frac{\partial^2}{\partial T^2}\left[\frac{F}{V}\right]=\sum_\sigma \frac{m_\sigma^* k_{F\sigma}}{6\hbar^2}k_B^2 T \tag{45}$$

in the limit of $T\to 0$, where $k_{F\sigma}$ is the Fermi wave number for the electrons with σ. We thus calculate m^* in the paramagnetic state (where $m^*=m_\uparrow^*=m_\downarrow^*$) and in the ferromagnetic state (where $m^*=m_\uparrow^*$) through the low-temperature behaviors of F_{xc}.

The temperature differentiations in Eq. (45) may be evaluated with the aid of

$$\frac{\partial^2 f_{xc}}{\partial\Theta^2}\simeq 2\delta f_{xc}(r_s,\Theta,\zeta)/\Theta^2 \tag{46}$$

where the increment,

$$\delta f_{xc}(r_s,\Theta,\zeta)=f_{xc}(r_s,\Theta,\zeta)-f_{xc}(r_s,0,\zeta)\ , \tag{47}$$

may be calculated through the coupling-constant integration of $\varepsilon_{int}(\Theta)-\varepsilon_{int}(0)$ as in Eq. (33). We remark in this connection that δf_{xc} is known to behave proportionally to $\Theta^2\ln\Theta$ for $\Theta\to 0$ in the Hartree-Fock approximation.[43,44] We have confirmed numerically, however, that the computed values of δf_{xc} are in fact proportional to Θ^2 for $\Theta\lesssim 0.2$ in the MCA calculation; Eq. (46) thus approaches a constant value in the limit of $\Theta\to 0$, leading to a correct Fermi-liquid behavior with a finite m^*. This departure of the MCA prediction from the Hartree-Fock one is a consequence of the Coulombic screening effect, and thus appears in the RPA calculation as well.[5,6] An analytic account of the low-temperature limiting behavior of F_{xc} in the RPA is given in the Appendix.

We evaluated m^* in the paramagnetic and ferromagnetic states by using the values of δf_{xc} calculated at $\Theta=0.1$. The results are depicted in Fig. 14, where some of the existing theoretical evaluations[29,45,46] in the paramagnetic state are also plotted.

The spin stiffness α_{xc} was calculated already through Eq. (39) in Sec. VI. The results for $\Theta=0$, 0.1, and 0.5 are listed in Table VI. The exchange contribution α_x to the

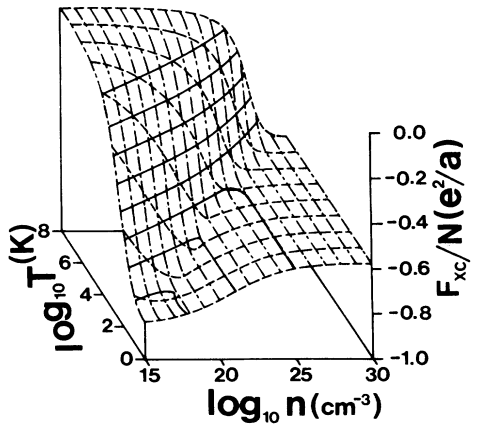

FIG. 13. Reduced excess free energy f_{xc} in the ferromagnetic state. Otherwise the same as in Fig. 12.

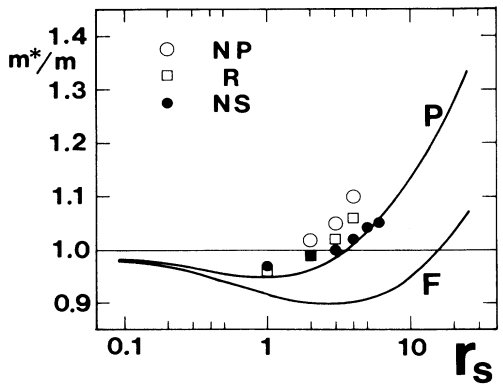

FIG. 14. The ratio of the effective mass m^* to the bare mass m. P refers to the MCA result in the ferromagnetic state; NP, the calculation by Pines and Nozières (Ref. 29); R, Rice (Ref. 45), NS, Ng and Singwi (Ref. 46).

TABLE VI. The correlation contribution to the spin stiffness in units of mRy for various values of r_s at $\Theta=0$, 0.1, and 0.5. The exchange contribution is given by $-407.3/r_s$, $-418.7/r_s$, and $-576.7/r_s$ at $\Theta=0$, 0.1, and 0.5, respectively.

r_s	$\Theta=0$	$\Theta=0.1$	$\Theta=0.5$
1	78.5	89.3	241.1
2	58.7	64.7	148.4
3	48.0	52.1	109.8
4	41.0	44.1	88.1
5	36.1	38.5	74.0
6	32.3	34.4	64.1
8	26.9	28.5	50.8
10	23.2	24.4	42.3

spin stiffness is expressed as

$$\frac{\alpha_x}{e^2/a}=-\tfrac{4}{9}a(\Theta)+\tfrac{2}{3}\Theta a'(\Theta)-\tfrac{4}{9}\Theta^2 a''(\Theta) \tag{48}$$

from Eqs. (12b) and (32), where $a(\Theta)$ is the exchange integral.[7] We thus find

$$\frac{\alpha_x}{e^2/a}\to-\frac{1}{3}\left[\frac{3}{2\pi}\right]^{2/3} \tag{49}$$

in the limit of complete degeneracy ($\Theta\to 0$) and

$$\frac{\alpha_x}{e^2/a}\to-\left[\frac{2}{3\pi^2}\right]^{1/3}\frac{1}{\Theta} \tag{50}$$

in the classical limit ($\Theta\to\infty$). The exchange contribution $\alpha_x/(e^2/a)$ has a minimum at a finite value of Θ.

The low-frequency and long-wavelength limit of the spin-response function, Eq. (8), which we shall denote as χ_-, is given by

$$\frac{1}{\chi_-}\equiv\frac{1}{\chi_-(0,0)}=-\frac{1}{n^2}\frac{\partial^2}{\partial\zeta^2}\left[\frac{F}{V}\right]. \tag{51}$$

The plasma-parameter dependence of χ_- can therefore be investigated on the basis of the free energies obtained in Sec. VI.

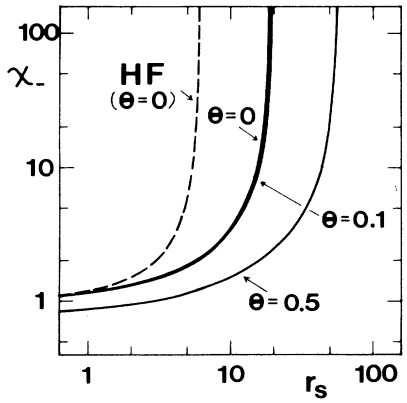

FIG. 15. Spin-response function χ_- in units of $-3n/2E_F$ at $\Theta=0$, 0.1, and 0.5. HF refers to the result in the Hartree-Fock approximation at $\Theta=0$ in which the correlation contribution to the free energy is neglected in Eq. (51).

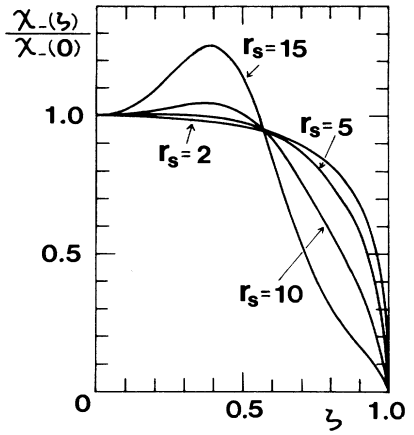

FIG. 16. Spin-response function $\chi_-(\zeta)$ plotted as a function of the spin polarization ζ for $r_s=2$, 5, 10, and 15 at the ground state ($\Theta=0$). $\chi_-(\zeta)$ is normalized by its paramagnetic value $\chi_-(0)$.

The r_s dependence of the spin-response function χ_- in the paramagnetic state is shown in Fig. 15 for $\Theta=0$, 0.1, and 0.5. Divergence of χ_- to infinity is found at a value of r_s; this divergence signals the onset of a transition from the paramagnetic state to the ferromagnetic state (see Sec. IX). We also plot in Fig. 16 the spin-polarization dependence of χ_- for various values of r_s at $\Theta=0$. It appears that χ_- has a maximum at a finite value of ζ for $r_s\gtrsim 5$, analogous to the case observed in the liquid ^{3}He.[42]

The isothermal compressibility κ is given by

$$\kappa^{-1}=n^2\frac{\partial^2}{\partial n^2}\left[\frac{F}{V}\right]. \tag{52}$$

With the aid of the parametrized expressions of F_{xc} constructed in Sec. VII, we calculate the values of κ in the paramagnetic and ferromagnetic states at various combinations of Θ and r_s (or Γ).

The Fermi-liquid parameters $F_l^{s(a)}$ are related to the thermodynamic quantities in a usual way.[29] To summarize the results in this section, we list in Table VII the values of F_0^s, F_0^a, and F_1^s for the degenerate paramagnetic electron liquid.

TABLE VII. Fermi-liquid parameters for the degenerate electron liquid in the paramagnetic state.

r_s	F_0^s	F_0^a	F_l^s
1	−0.214	−0.176	−0.147
2	−0.381	−0.265	−0.114
3	−0.554	−0.329	−0.030
4	−0.747	−0.389	0.036
5	−0.956	−0.444	0.102
6	−1.179	−0.495	0.168
10	−2.201	−0.676	0.399
20	−5.444	−1.039	0.843

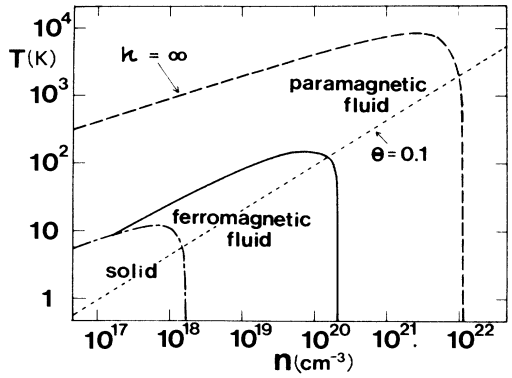

FIG. 17. Phase diagram of the electron liquid on the number density vs temperature plane. The dashed curve corresponds to the condition at which the isothermal compressibility κ on the paramagnetic fluid diverges to infinity; the solid curve describes the boundary between the paramagnetic and ferromagnetic fluid phases; the dot-dashed curve represents an interpolation between the crystallization conditions, $\Gamma = 178$ (Ref. 9) in the classical limit and $r_s = 100$ (Ref. 10) in the degenerate limit.

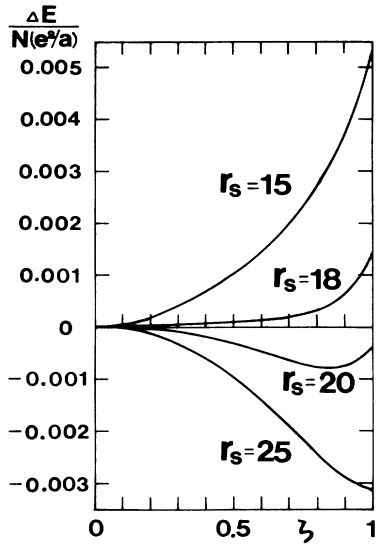

FIG. 19. The difference between the ground-state energies in an arbitrarily spin-polarized state and in the paramagnetic state, calculated in the MCA scheme.

IX. PHASE DIAGRAM

As the numerical values in Table VII illustrate, the Fermi-liquid parameters F_0^s and F_0^a in the paramagnetic phase take on values below -1 at $r_s \simeq 5$ and at $r_s \simeq 20$, respectively; these may imply thermodynamic instabilities.[29] We study in this section those phase boundaries associated with the compressibility and spin-susceptibility anomalies in the finite-temperature electron system.

In the ground state, the isothermal compressibility κ of the paramagnetic electron liquid diverges to infinity at $r_s = 5.2$ in the MCA calculation; the compressibility becomes negative for $r_s > 5.2$. We find analogous divergence of κ in the classical OCP (Ref. 9) at $\Gamma = 3.1$. We depict in Fig. 17 the curve representing $\kappa = \infty$ on the density-temperature plane. derived from the equations of state as obtained in Secs. VI and VII. Such a negativeness of the compressibility does not immediately imply a thermodynamic instability of the system, however, because of the assumed, rigid background of neutralizing charges in the electron liquid.[1,47] We shall consider in Sec. X some of the physical consequences arising from finiteness of the compressibility in the ionic background.

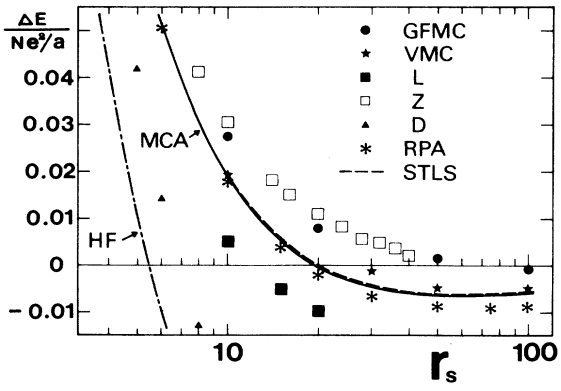

FIG. 18. The difference $\Delta E = E(\zeta = 1) - E(\zeta = 0)$ of the ground-state energy between the ferromagnetic and paramagnetic phases in units of Ne^2/a. MCA refers to the present calculation; STLS, the calculation based on the integral equations by Singwi *et al.* (Ref. 34); HF, the Hartree-Fock approximation, Eq. (32); RPA, the random-phase approximation (Ref. 11); *D*, Dunaevskii (Ref. 39); *Z*, Zabolitzky (Ref. 49); *L*, Lantto (Ref. 48); VMC, the variational Monte Carlo (Ref. 38); GFMC, the Green's-function Monte Carlo (Ref. 10).

The divergence of the spin susceptibility, on the other hand, does imply a phase transition into ferromagnetic state. As Eq. (51) shows, $\chi_- \to \infty$ implies an enormous enhancement of spin-density fluctuations. The transition point may be determined through comparison of the Helmholtz free energies between the paramagnetic ($\zeta = 0$) and ferromagnetic ($\zeta = 1$) states. The differences between those free energies in the MCA, STLS, and Hartree-Fock calculations are plotted in Fig. 18 as functions of r_s at $\Theta = 0$. For comparison we have also plotted in the same figure the results obtained earlier by a number of investigators.[10,11,38,39,48,49] We observe in Fig. 18 that the r_s values of the transition hitherto predicted scatter widely between $r_s = 5.45$ (Hartree-Fock) and 75 (GMFC); the MCA prediction at $r_s = 19.6$ and the STLS prediction at $r_s = 20.1$ fall somewhere between them.

To see detailed features of the transition, we depict in Fig. 19 the spin-polarization dependence of the ground-state energies calculated in the MCA scheme above and below the ferromagnetic transition point. The metastability of the transition predicted in the Hartree-Fock calculations[50] does not appear here. We also note in Fig. 19 that a state with intermediate value of spin polarization ($0 < \zeta < 1$) can be thermodynamically stable at $r_s \simeq 20$.

Such an intermediate polarization does not appear in the RPA calculation.[11]

The foregoing arguments on the ferromagnetic transition can be extended to the systems with finite temperatures. Comparing the free energies between the paramagnetic and ferromagnetic states, we have derived the phase boundary curve depicted in Fig. 17.

At still lower densities and temperatures, the electrons may undergo a transition into a crystalline state (i.e., the Wigner crystallization). In Fig. 17, we have drawn such a boundary curve as an interpolarization between $\Gamma=178$ for $\Theta \gg 1$ (Ref. 9) and $r_s=100$ for $\Theta \ll 1$ (Ref. 10).

There exist possibilities of other anomalies associated with the onset of a charge-density-wave[51] (CDW) instability and of a spin-density-wave[25] (SDW) instability, signaled by the conditions

$$1-v(k)[1-G(k)]\chi_0(k,0)=0 \quad \text{(CDW)}, \tag{53}$$

$$1+v(k)G_1(k)\chi_0(k,0)=0 \quad \text{(SDW)} \tag{54}$$

at nonzero values of k. In the present MCA analyses, such instabilities leading to inhomogeneous states are not predicted at relevant plasma parameters in a three-dimensional electron liquid; possibilities in a two-dimensional electron liquid are under investigation.

X. ELECTRON-ELECTRON INTERACTION

According to Kukkonen and Overhauser,[52,53] the spin-dependent interactions between two conduction electrons in metallic substances may be expressed as

$$V_{\sigma\tau}(k)=\frac{4\pi e^2}{k_F^2}\left[\frac{\omega_k^2-\omega_0^2}{\omega^2-\omega_k^2}L(k)+N(k)+(2\delta_{\sigma\tau}-1)M(k)\right] \tag{55}$$

in the paramagnetic state, where

$$L(k)=\frac{k_F^2/k^2}{[1+v(k)G(k)\chi_0(k,0)]\{1-v(k)[1-G(k)]\chi_0(k,0)]\}}, \tag{56}$$

$$N(k)=\left[\frac{k_F}{k}\right]^2\frac{1-v(k)G(k)[1-G(k)]\chi_0(k,0)}{1-v(k)[1-G(k)]\chi_0(k,0)}, \tag{57}$$

$$M(k)=\left[\frac{k_F}{k}\right]^2\frac{v(k)G_-(k)^2\chi_0(k,0)}{1+v(k)G_-(k)\chi_0(k,0)}. \tag{58}$$

The ω dependence in Eq. (55) is assumed to stem only from the phonon coordinates, so that the electrons make a static response with $\chi_0(k,0)$ and $G_{\sigma\tau}(k)$. The frequency ω_k denotes the characteristic frequency of the phonon; $\omega_0=s_0k$ with s_0 representing the sound velocity of the ion background in the absence of Coulomb forces.

The electron-electron interaction in the ferromagnetic (spin-aligned) state may be analogously obtained as

$$V_1(k)=\frac{4\pi e^2}{k_F^2}\left[\frac{\omega_k^2-\omega_0^2}{\omega^2-\omega_k^2}L(k)+N(k)\right]. \tag{59}$$

In Eqs. (56), (57), and (59), k_F and $\chi_0(k,\omega)$ should be evaluated appropriately for the electrons in the spin-aligned state.

Physically, the terms of Eqs. (55) and (59) involving $L(k)$ describe those parts of the electron interactions induced by the lattice vibrations or phonons. If we replace the ions with a rigid, uniform background of positive charges, those terms identically vanish. The terms involving $N(k)$ represent the spin-symmetric parts of the electron interactions independent of the lattice vibrations. The term in Eq. (55) involving $M(k)$ describes the spin-antisymmetric part of the electron interactions. We may define a net interaction between electrons with parallel spins as

$$P(k)=N(k)+M(k) \tag{60}$$

in the paramagnetic state.

We have calculated $L(k)$, $N(k)$, and $M(k)$ for various combinations of Θ and r_s in the MCA scheme. $G_{\sigma\tau}(k)$ have been modified slightly through

$$\tilde{G}(k)=\left[\left(\frac{\gamma_0^{\rm EOS}}{\gamma_0^{\rm LFC}}-1\right)\exp\left(-\frac{k^2}{k_c^2}\right)+1\right]G(k), \tag{61}$$

$$\tilde{G}_-(k)=\left[\left(\frac{\gamma_-^{\rm EOS}}{\gamma_-^{\rm LFC}}-1\right)\exp\left(-\frac{k^2}{k_c^2}\right)+1\right]G_-(k), \tag{62}$$

so that the compressibility and spin-susceptibility sum rules are satisfied exactly; the characteristic wave number k_c has been chosen as $k_c=2k_F$.

We plot in Fig. 20 the values of $L(k)$ computed in the present scheme for $r_s=4$, 6, and 18 at $\Theta=0.1$ in the paramagnetic state. Since the long-wavelength limit of $1+v(k)G(k)\chi_0(k,0)$ takes on a value inversely proportional to κ owing to the compressibility sum rule, the magnitude of the phonon-induced interaction is enhanced drastically in the long-wavelength regime as the compressibility anomaly ($\kappa\to\infty$) at $r_s\simeq 5$ is approached; across the anomaly, $L(0)$ changes its sign from positive to negative through infinity. When $\kappa<0$, $L(k)$ starts with a negative value at $k=0$, increases its magnitude with k, and diverges to negative infinity at a finite value of k, where $L(k)$ turns over to positive infinity and then decreases

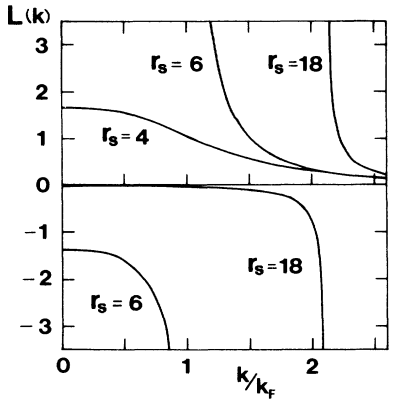

FIG. 20. Phonon-induced electron-interaction function $L(k)$ for $r_s=4$, 6, and 18 at $\Theta=0.1$ in the paramagnetic state.

monotonically as k further increases. Correspondingly the phonon-induced electron interactions exhibit remarkable k dependence in its sign and magnitude.

The function $N(k)$ takes on positive definite values, so that this part of the interactions remains repulsive. On the other hand, the function $M(k)$ is negative definite in the paramagnetic state, so that it makes an attractive interaction between electrons with parallel spins, due physically to negativeness of the interaction energy associated with the exchange hole. We plot in Fig. 21 the values of $P(k)$ at $r_s=6$ and 18 in the paramagnetic state and the values of $N(k)$ at $r_s=25$ in the ferromagnetic state at $\Theta=0.1$. Since the long-wavelength limit of $1+v(k)G_-(k)\chi_0(k,0)$ takes on a value inversely proportional to the spin susceptibility[2] owing to the spin-susceptibility sum rule, the magnitude of the spin-antisymmetric part of the electron interactions is enhanced enormously in the long-wavelength regime as the spin-susceptibility anomaly ($\chi_- \to \infty$) at $r_s \simeq 22$ is approached. We thus find in Fig. 21 that a strong attractive interaction between electrons with parallel spins appears

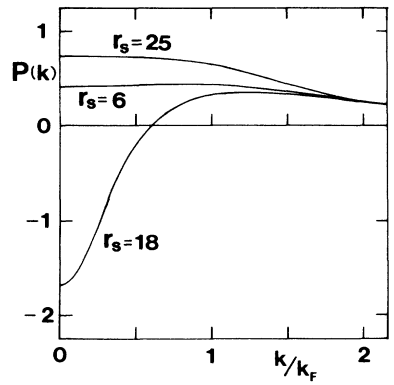

FIG. 21. Intrinsic electron-interaction function $P(k)$ between parallel spins for $r_s=6$, 18, and 25 at $\Theta=0.1$. Note that $P(k)=N(k)$ in the ferromagnetic state (i.e., at $r_s=25$).

in the long-wavelength regime at $r_s=18$. Such an attractive interaction does not exist at $r_s=25$, however, where the system is in the spin-aligned state.

The features of the electron interactions elucidated thus far along $\Theta=0.1$ remain virtually the same for $\Theta<0.1$, as the phase boundary curves in Fig. 17 form vertical line (n: constant) there. We may thus expect that those remarkable changes in the spin-dependent and phonon-induced electron-electron interactions across the phase boundaries have significant consequences in the electronic transport in metallic substances over a wide range of density and temperature parameters.

XI. CONCLUSION

We have analyzed the spin-dependent static correlations in electron liquids on the basis of the MCA scheme as applied to the multicomponent charged system. The scheme has been shown to provide as self-consistent description of the thermodynamic properties over a wide range of density, temperature, and spin polarization; the accuracy of the scheme has been examined through comparison with the MC data. The parametrized expressions for the free energies are derived as functions of plasma parameters Θ, r_s, and ζ; Fermi-liquid parameters are thereby calculated. Phase boundary curves are drawn on the n-T plane, representing the conditions for divergence of the isothermal compressibility and the spin susceptibility in the electron liquid. It is shown quantitatively that the signs and magnitude of the spin-dependent and phonon-induced electron interactions exhibit remarkable changes across the phase boundary in the metallic electrons.

ACKNOWLEDGMENTS

We thank our colleagues, Dr. H. Iyetomi, X.-Z. Yan, A. Nakano, and S. Ogata, for useful discussions on this and related problems. This work was supported in part through Grants-in-Aid for Scientific Research provided by the Japanese Ministry of Education, Science, and Culture. One of us (S.T.) acknowledges receipt of partial support from the Japan Society for the Promotion of Science.

APPENDIX: LOW-TEMPERATURE BEHAVIOR OF EXCESS FREE ENERGY

In the Hartree-Fock approximation, the excess free energy F_{xc} and hence the specific heat C_v have a logarithmic singularity in the limit of low temperature.[43,44] It has been demonstrated through numerical calculations,[5,6] however, that such a singularity disappears when the Coulomb correlation or the screening effect is appropriately taken into account. In this appendix we show explicitly that the logarithmic singularity indeed disappears in the RPA.

We begin with the RPA expression for the excess free energy F_{xc} in the paramagnetic state.[7] The increment of F_{xc} due to an increase of the temperature from $T=0$ may be expressed as

$$\delta F_{\rm xc}=-\frac{Vk_BT}{2}\int\frac{d\mathbf{k}}{(2\pi)^3}\sum_{l=-\infty}^{\infty}\frac{v(k)\delta\chi_0(k,z_l)}{1-v(k)\chi_0(k,z_l)}\ , \quad \text{(A1)}$$

where $\delta\chi_0$ denotes the increment in the free-particle polarizability,[2] $z_l=2\pi ilk_BT/\hbar$, and l denotes integers.

We adopt a static-screening approximation, so that $\chi_0(k,z_l)$ in the denominator of Eq. (A1) is replaced by its static value $\chi_0(k,0)$. We next note an identity,

$$-\frac{k_BT}{n}\sum_{l=-\infty}^{\infty}\chi_0(k,z_l)=1-\frac{2}{n}\int\frac{d\mathbf{q}}{(2\pi)^3}f(\mathbf{q})f(\mathbf{q}+\mathbf{k})\ , \quad \text{(A2)}$$

where $f(k)$ is the Fermi distribution function.[2] We thus find

$$\delta F_{\rm xc}=-2V\int\frac{d\mathbf{k}}{(2\pi)^3}\int\frac{d\mathbf{q}}{(2\pi)^3}\frac{4\pi e^2}{|\mathbf{k}-\mathbf{q}|^2+k_{\rm TF}^2}f(k)\delta f(q)\ , \quad \text{(A3)}$$

where δf denotes the increment of f due to the increase of temperature and $k_{\rm TF}=(6\pi ne^2/E_F)^{1/2}$ is the Thomas-Fermi screening wave number.

Assuming $\Theta\ll 1$, we may approximate $f(k)$ and $\delta f(q)$ by their limiting expressions.[44] We can thus carry out the $\mathbf{k}$ integration in Eq. (A3).

If we set $k_{\rm TF}=0$ in the resulting equation, we recover the Hartree-Fock expression[44] for $\delta F_{\rm xc}$. Expanding the integrand around $q=k_F$ and carrying out the q integration, we then find

$$\delta F_{\rm xc}=V\frac{e^2m^2(k_BT)^2}{6\pi\hbar^4}\ln\left[\frac{E_F}{k_BT}\right]+O(T^2,e^2)\ , \quad \text{(A4)}$$

the leading term in the Hartree-Fock approximation.[43,44]

Such a logarithmic singularity in the low-temperature regime has stemmed from overlapping of the Coulomb singularity in the long-wavelength limit and the Fermi-distribution singularity at the Fermi surface; it may removed if the screening wave number is kept finite (i.e., $k_{\rm TF}\neq 0$). In fact, expanding the integrand around $q=k_F$ and carrying out the q integration, we obtain

$$\delta F_{\rm xc}=-V\frac{e^2m^2(k_BT)^2}{12\pi\hbar^4}\ln\left[\left[\frac{4}{9\pi}\right]^{1/3}\frac{r_s}{\pi}\right]+O(T^2,e^2)\ . \quad \text{(A5)}$$

The logarithmic singularity has thus been transformed from $\ln T$ to $\ln r_s$, so that the specific heat is a well-behaved quantity in the low-temperature limit. The effective mass calculated with Eq. (A5) is[54]

$$\frac{m^*}{m}=1+\left[\frac{4}{9\pi}\right]^{1/3}\frac{r_s}{2\pi}\ln\left[\left[\frac{4}{9\pi}\right]^{1/3}\frac{r_s}{\pi}\right]+O(r_s)\ . \quad \text{(A6)}$$

[1] S. Ichimaru, Rev. Mod. Phys. **54**, 1017 (1982).

[2] S. Ichimaru, H. Iyetomi, and S. Tanaka, Phys. Rep. **149**, 91 (1987).

[3] G. Gouedard and C. Deutsch, J. Math. Phys. **19**, 32 (1978); N. R. Arista and W. Brandt, Phys. Rev. A **29**, 1471 (1984).

[4] U. Gupta and A. K. Rajagopal, Phys. Rep. **87**, 259 (1982).

[5] F. Perrot and M.W. C. Dharma-wardana, Phys. Rev. A **30**, 2619 (1984).

[6] D. G. Kanhere, P. V. Panat, A. K. Rajagopal, and J. Callaway, Phys. Rev. A **33**, 490 (1986).

[7] S. Tanaka, S. Mitake, and S. Ichimaru, Phys, Rev. A **32**, 1896 (1985); S. Tanaka and S. Ichimaru, J. Phys. Soc. Jpn. **55**, 2278 (1986).

[8] R. G. Dandrea, N. W. Ashcroft, and A. E. Carlsson, Phys. Rev. B **34**, 2097 (1986).

[9] W. L. Slattery, G. D. Doolen, and H. E. DeWitt, Phys. Rev. A **21**, 2087 (1980); **26**, 2255 (1981); see also, S. Ogata and S. Ichimaru, Phys. Rev. A **36**, 5451 (1987).

[10] D. M. Ceperley and B. J. Alder, Phys. Rev. Lett. **45**, 566 (1980).

[11] For parametrization of the MC data in Ref. 10, see S. H. Vosko, L. Wilk, and M. Nusair, Can. J. Phys. **58**, 1200 (1980).

[12] K. S. Singwi and M. P. Tosi, in *Solid State Physics,* edited by H. Ehrenreich, F. Seitz, and D. Turnbull (Academic, New York, 1981), Vol. 36, p. 177.

[13] S. Jüngst, B. Knuth, and F. Hensel, Phys. Rev. Lett. **55**, 2160 (1985); J. P. Hernandez, *ibid.* **57**, 3183 (1986).

[14] M. A. Bredig, in *Molten Salt Chemistry,* edited by M. Blander (Interscience, New York, 1964), p. 367; G. Chabrier and J.-P. Hansen, J. Phys. C **18**, L757 (1985).

[15] K. A. Brueckner and S. Jorna, Rev. Mod. Phys. **46**, 325 (1974); F. Perrot and M. W. C. Dharma-wardana, Phys. Rev. A **29**, 1378 (1984).

[16] J. N. Bahcall, W. F. Huebner, S. H. Lubow, P. D. Parker, and R. K. Ulrich, Rev. Mod. Phys. **54**, 767 (1982); H. Iyetomi and S. Ichimaru, Phys. Rev. A **34**, 3203 (1986).

[17] A preliminary account of those results has been reported in S. Ichimaru and S. Tanaka, Phys. Rev. B **36**, 6182 (1987).

[18] K. Tago, K. Utsumi, and S. Ichimaru, Prog. Theor. Phys. **65**, 54 (1981).

[19] X.-Z. Yan and S. Ichimaru, J. Phys. Soc. Jpn. **56**, 3853 (1987).

[20] D. Pines, in *Quantum Fluids,* edited by D. F. Brewer (North-Holland, Amsterdam, 1966), p. 257.

[21] P. Vashishta and K. S. Singwi, Solid State Commun. **13**, 901 (1973).

[22] P. Vashishta, P. Bhattacharyya, and K. S. Singwi, Phys. Rev. B **10**, 5108 (1974).

[23] S. Ichimaru, S. Mitake, S. Tanaka, and X.-Z. Yan, Phys. Rev. A **32**, 1768 (1985).

[24] R. Lobo, K. S. Singwi, and M. P. Tosi, Phys. Rev. **186**, 470 (1969).

[25] K. Utsumi and S. Ichimaru, Phys. Rev. B **28**, 1792 (1983).

[26] J. C. Kimball, Phys. Rev. A **7**, 1648 (1973).

[27] T. Kawazoe, H. Yasuhara, and M. Watabe, J. Phys. C **10**, 3293 (1977).

[28] G. Vignale and K. S. Singwi, Phys. Rev. B **31**, 2729 (1985).

[29] D. Pines and P. Nozières, *The Theory of Quantum Liquids* (Benjamin, New York, 1966), Vol. 1.

[30] D. Pines, *Elementary Excitations in Solids* (Benjamin, New York, 1964).

[31]S. Ichimaru, *Basic Principles of Plasma Physics* (Benjamin, Reading, Mass., 1973).
[32]S. Ichimaru, Phys. Rev. A **2**, 494 (1970).
[33]H. Iyetomi, Prog. Theor. Phys. **71**, 427 (1984).
[34]K. S. Singwi, M. P. Tosi, R. H. Land, and A. Sjölander, Phys. Rev. **176**, 589 (1968).
[35]K. Utsumi and S. Ichimaru, Phys. Rev. B **22**, 5203 (1980).
[36]A. L. Fetter and J. D. Walecka, *Quantum Theory of Many-Particle Systems* (McGraw-Hill, New York, 1971).
[37]U. von Barth and L. Hedin, J. Phys. C **5**, 1629 (1972).
[38]D. M. Ceperley, Phys. Rev. B **18**, 3126 (1978).
[39]S. M. Dunaevskii, Fiz. Tverd. Tela (Leningrad) **20**, 3565 (1978) [Sov. Phys.—Solid State **20**, 1483 (1978)].
[40]K. S. Singwi, A. Sjölander, M. P. Tosi, and R. H. Land, Phys. Rev. B **1**, 1044 (1970).
[41]J. F. Springer, M. A. Pokrant, and F. A. Stevens, Jr., J. Chem. Phys. **58**, 4863 (1973); B. Brami, J.-P. Hansen, F. Joly, Physica A **95**, 505 (1979).
[42]K. S. Bedell and C. Sanchez-Castro, Phys. Rev. Lett. **57**, 854 (1986).
[43]A. Wasserman, T. J. Buckholtz, and H. E. DeWitt, J. Math. Phys. **11**, 477 (1970).
[44]B. Horovitz and R. Thieberger, Physica **71**, 99 (1974).
[45]T. M. Rice, Ann. Phys. (N.Y.) **31**, 100 (1965).
[46]T. K. Ng and K. S. Singwi, Phys. Rev. B **34**, 7738 (1986); **34**, 7743 (1986).
[47]P. Viellefosse and J.-P. Hansen, Phys. Rev. A **12**, 1106 (1975).
[48]J. L. Lantto, Phys. Rev. B **22**, 1380 (1980).
[49]J. G. Zabolitzky, Phys. Rev. B **22**, 2353 (1980).
[50]A. B. Lidiard, Proc. Phys. Soc. London, Sect. A **64**, 814 (1951).
[51]H. Iyetomi, K. Utsumi, and S. Ichimaru, Phys. Rev. B **24**, 3226 (1981).
[52]C. A. Kukkonen and A. W. Overhauser, Phys. Rev. B **20**, 550 (1979).
[53]See also, C. A. Kukkonen and J. W. Wilkins, Phys. Rev. B **19**, 6075 (1979); A. H. MacDonald, Can. J. Phys. **60**, 710 (1982).
[54]M. Gell-Mann, Phys. Rev. **106**, 369 (1957).